ISSN: 2148-9173 **Vol: 9 Issue:1 January 2022**

International Journal of Environment and Geoinformatics (IJEGEO) is an international, multidisciplinary, peer reviewed, open access journal.

A Review of UHI formation over changing climate and its impacts on Urban Land Use and Environments and Adaptation Measures

Sumanta DAS

Abstracting and Indexing: TR DIZIN, DOAJ, Index Copernicus, OAJI, Scientific Indexing Services, International Scientific Indexing, Journal Factor, Google Scholar, Ulrich's Periodicals Directory, WorldCat, DRJI, ResearchBib, SOBIAD

International Journal of Environment and Geoinformatics 9(1):064-073 (2022)

Review Article

A Review of UHI formation over changing climate and its impacts on Urban Land Use and Environments and Adaptation Measures

Sumanta Das

West Bengal Disaster Management Department, Govt. of West Bengal, West Bengal-711102, India

* Corresponding author: Name Surname
E-mail: sumanvu_27@yahoo.co.in

Received 17.05.2021
Accepted 15.09.2021

How to cite: Das (2022). A Review of UHI formation over changing climate and its impacts on Urban Land Use and Environments and Adaptation Measures. *International Journal of Environment and Geoinformatics (IJEGEO)*, 9(1): 064-073. doi. 10.30897/ijegeo.938231

Abstract

Climate change and associated global warming adversely impact urban environments, which leads to the increasing of land surface temperature (LST) and the formation of urban heat islands (UHI). In this study, the author has attempted to present current understandings of UHI formation over changing climate and its probable impacts on urban land use and environmental risks. The review provides a thorough understanding of the UHI and how this impacts urban communities, land use, and environments. In addition, the author has also addressed the quantification process of UHI in the Geospatial platform which helps monitor, assess, and predict the environmental risks at a local scale. The study demonstrated the advantages of earth observation data and Geo-Spatial technologies to detect and monitor the UHI over the temporal scale and a clear understanding of spatial data processing for quantification of UHI. The author finally suggested some best possible adaptation measures of UHI that can assist urban planners and policy makers to build resilient urban communities.

Keywords: UHI,LST, Geo-spatial technologies, UR, Adaptation

Introduction

Rapid and unplanned urbanization of cities and a concomitant reduction in vegetation result in an increased rise in temperature compared to non-urban areas. Rapid urbanization combined with changes in land use pattern during several decades led to about 1.8°C warmings of major metropolitan cities in India compared with surrounding non-urban areas (called the urban heat island effect), Study (Kaya et al., 2012; Prasad, 2017) revealed that the increase in urbanization has been rapid at 83% in the last 15 years. This has led to about 89% decrease in dense vegetation, about 2% decrease in water bodies, and a nearly 83% decrease in crop fields during the same period. The decrease in crop areas could either be due to urbanization or fields remaining fallow. These changes have led to an increase in the urban heat island effect. The major metropolitan cities and adjoining areas in India have witnessed major changes due to the expansion of the city, leading to the warming of the city. Rapid urbanization and subsequently encroachment of natural vegetation lead to a negative impact on the thermal and radiative properties of the surface and make cities hotter than surrounding non-urban areas. With heavily built-up areas and concrete structures, most cities in India and the world are warmer than surrounding non-urban areas due to the urban heat island effect (Prasad, 2017; Şekertekin et al., 2016; Burak et al., 2004).

Urban heat islands (UHI) are part of a metropolitan area that is significantly warmer than its surrounding areas (Marko et al., 2016). Rapid urban shift often results in a series of urban environmental problems (Akyüz, 2021). Urbanization includes the removal of vegetation cover to construct new highly reflective surfaces (parking lots, rooftops, roads, etc). This results in high thermal radiation at the surface producing UHI. The main cause of this UHI is the faster rate of cooling of the open spaces around cities when compared with the rate of nocturnal cooling of the densely built-up areas. The larger and denser the city, the greater is the difference in air temperature between the city center and the surrounding rural areas. The urban heat island grows with time. These thermal changes contribute to the change in flora; fauna, increased cooling load requirements in summer, increased discomfort to human health (heat stroke), use of air-conditioning increases heat burden externally along with increased GHG emission.

As population centers grow in size from village to town to city, they tend to have a corresponding increase in average temperature (Giannini et al., 2015; Ülker et al., 2018, 2020). This consequently increases building energy demand for air-conditioning in warmer countries like tropical regions. This increase in energy demand could result in not only an additional generation of anthropogenic heat but also further intensification of heat islands themselves (Snyder et al., 1998).

Quantification of the impacts of UHI is, therefore, an important component in urban planning as well as emission reduction strategies. Studies (Brivio et al., 2006; Sobrino et al., 1990) have shown the emergence of the urban heat island phenomenon in the past decade. Changes in urban land use and land cover (LULC), due to increasing population and infrastructure pressures for rapidly growing megacities, play an important role in the development of urban heat islands. Such a rapidly increasing population in megacities is associated with somewhat similar growth rates in vehicular population, residential and commercial complexes, industries, and other infrastructure resulting in significant changes in LULC and an increase in anthropogenic heat emissions. All these changes occur for generating several UHI pockets and shift in the dynamics of the urban heat island phenomenon. While the increasing temperature can be the significant reason behind global warming, which in turn, might affect the urban climate?

The magnitude of the urban heat island effect varies both spatially and temporally. In general, the heat island effect is maximized on clear days, when incoming solar radiation is high and nighttime cooling proceeds most slowly (Sobrino et al., 2004). Thus, the complex problem can be solved through a sound decision-making system where the amalgamation of Remote Sensing data and GIS techniques solely stands as the sound analyzer with a futuristic approach. The remote sensing technique with its repetitive and synoptic coverage with high-resolution data helps to identify and monitor the environmental degradation which is the combined effects of UHI. Over the past few years, remotely sensed data have been widely used to study the land use and land cover changes and environmental risks assessment associated with urban growth, and to retrieve land surface biophysical parameters, such as vegetation abundances, built-up indices, and land surface temperatures; those are good indicators of conditions of urban eco-system. Greenness or vegetation abundance to study eco-environment plays a crucial role in the exchange of material and energy over the land surface (Carlson and Ripley, 1997).

Accurate mapping and monitoring of spatio-temporal dynamics of vegetation in the urban area are essential to understand urban ecosystems, including its role in mitigating air pollution and reducing the urban heat island effect. Impervious land surface, as one of the most important land cover types and characteristics of urban/suburban environments, is known to affect urban surface temperatures. However, accurate estimation of land surface temperatures from remote sensing images is a challenge due to the high probability of mixed pixels of other urban classes and thus, this may not produce satisfactory accuracy in outcomes. To quantify the UHI effect, accurate retrieval of land surface temperature is important from earth observation data over a while. Near-surface soil moisture (SM) index is also an important parameter for UHI quantification and can be measured by remote sensing satellite data. The quantification process of the indicators of the UHI, such as land surface temperatures, vegetation abundance, soil moisture, surface wetness, impervious surface index, etc can be done using various multivariate statistical techniques to determine the correlation between parameters. Based on the observation and outcomes, a suitable decision with adaptation measures can be made towards urban resilience.

Urban Heat Islands – Effects

The urban heat island (UHI) effect is widely recognized as a heat accumulation phenomenon, which is the most obvious characteristic of urban climate caused by urban construction and human being activities (Yang, 2014; Oke, 1973). In the early 19th century, scholar Lake Howard firstly measured and discussed the UHI effect when studying urban climate in London, England. Since then, many scholars around the world have conducted deep research on the characteristics of the UHI effect (Arnfield, 2003; Oke and Maxwell, 1975), reaching that the UHI effect has a close relationship with urban heat release, properties, and structure of the underlying surface, vegetation coverage, population density and weather conditions. Meanwhile, the scale and intensity of the UHI effect will be increasingly serious with the ongoing urbanization.

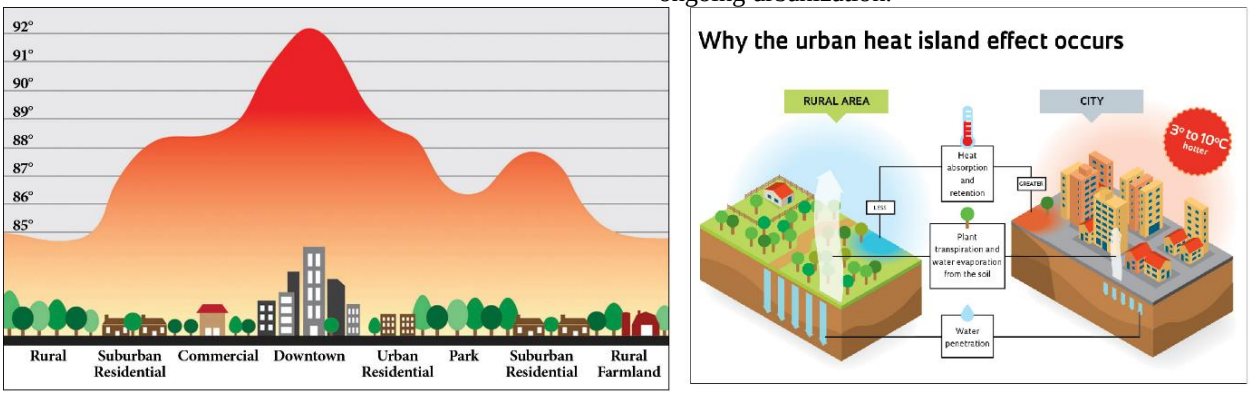

(a) (b)

Fig. 1: Urban Heat Island Profile in Rural to Urban areas (a) and causes of UHI (b)

Urban temperature, especially surface temperature, is the energy balance center of the urban surface and one of the most important factors affecting urban climate, regulating and controlling various ecological processes (Blocken et al., 2007; Pickett et al., 2008). However, the increasingly intensive urbanization has led to the

constant increase of surface temperature, definitely resulting in the altering of urban resource and energy flow. More importantly, the structure and function of the urban ecological system will also be changed, affecting urban residents' health. In addition, the UHI effect has received great attention from urban meteorologists. Figure 1 (a) & (b) shows the UHI profile and causes respectively (Arnfield, 2003; Oke and Maxwell, 1975).

Cities with variable landscapes and climates can exhibit temperatures several degrees higher than their rural surroundings (i.e. UHI effect), a phenomenon which if increases in the future, may result in a doubling of the urban to the rural thermal ratio in the following decades. Hence, assessment of the UHI and strategies to implement its mitigation is becoming increasingly important for government agencies and researchers of many affected countries.

As it would be expected, the characteristic inclination towards warming of urban surfaces is exacerbated during hot days and heatwaves, which reinforces the air temperature increase, particularly in ill-ventilated outdoor spaces or inner spaces of residential and commercial buildings with poor thermal isolation. This increases the overall energy consumption for cooling (i.e. refrigeration and air-conditioning), hence increasing the energy production by power plants, which leads to higher emissions of heat-trapping greenhouse gases such as carbon dioxide, as well as other pollutants such as sulfur dioxide, carbon monoxide, and particulate matter. Furthermore, the increased energy demand means more costs to citizens and governments, which in large metropolitan areas may induce significant economic impacts. On the other hand, UHIs promote high air temperatures that contribute to the formation of ozone precursors, which combined photochemically produce ground-level ozone.

A direct relationship has been found between the UHI intensity peaks and heat-related illness and fatalities, due to the incidence of thermal discomfort on the human cardiovascular and respiratory systems (Pickett et al., 2008). During extreme weather events such as heatwaves, the urban heat island has the potential to prevent the city from cooling down, maintaining night-time temperatures at a level that affects human health and comfort. Heatstroke, heat exhaustion, heat syncope, and heat cramps are some of the main stress events, while a wide number of diseases may become worse, particularly in the elderly and children. Similarly, respiratory and lung diseases are related to high ozone levels induced by heat events. Studies (Pickett et al., 2008; Khan and Chatterjee 2016) carried out in several cities of the United States such as Atlanta, New York, Chicago, and Washington, have shown that urban-induced precipitation and thunderstorm events are mainly initiated by the UHI. Other meteorological impacts of the UHI are associated with reductions in snowfall frequencies and intensities, as well as reductions in the diurnal and seasonal range of freezing temperatures. Lastly, high temperatures may produce physiological and phonological disturbances on ornamental plants and urban forests.

Climate change and heat island effects on human health and mortality

Climate change and changes in land use have similar impacts on society's health and living. Both changes focus on the deterioration of ecosystem dynamics and its stabilization. Global climate change may affect human health and nutrition resources. Human health is affected by climate change through biogeochemical interactions and the presence of biological responses towards the climate and the atmospheric composition. The formation of heat stress through the heatwave amongst humans may lead to more serious illnesses, such as heat stroke. Increased temperature can also amplify air pollution concentrations which lead to the formation of major cardiorespiratory allergies. Pollution also influences the climate of the city. Pollution particles reflect solar radiation, leading to a decrease in solar energy reaching the surface. Heat islands have been recorded as major urbanization effects.

In Situ Observation for Analyses of Urban Heat Islands – Perspectives from India

The main purpose of the in situ temperature, as well as humidity observation, is to detect the diurnal variation of vertical air temperature and surface temperature with an urban concrete surface and suburban open surface, to get the relationship between them. Based on the relationship, the daily surface temperatures can be approximated by air temperature at peak 14:00 hrs and daily lowest temperatures. These data and the relationship are used to determine the top boundary temperatures in numerical simulation. Meanwhile, the air temperature, surface temperature, vertical temperatures, and air moisture of two sites were recorded every day during the study period to compare with simulation results (Khan and Chatterjee 2016).

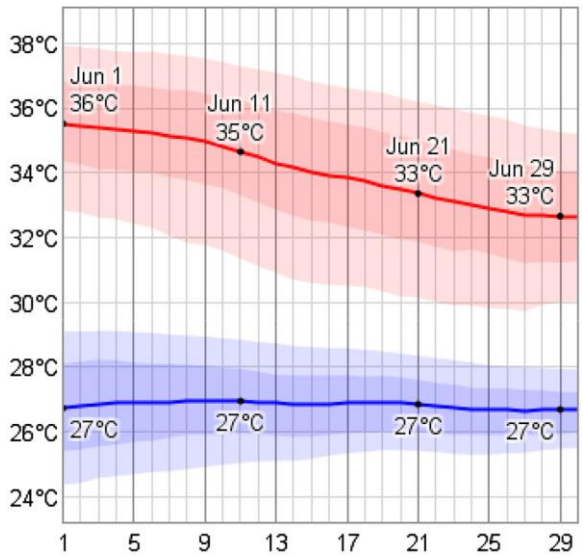

Fig. 2: The daily average low (blue) and high (red) temperature (Khan and Chatterjee 2016)

The month of June is characterized by falling daily high temperatures, with daily highs ranging from36 to 33°C over the month, exceeding 38°C or dropping below 30°C only one day in ten. Daily low temperatures are around 27°C, falling below 24°C or exceeding 29 °C only one day in ten in Figure 2 (Khan and Chatterjee 2016).

The relative humidity typically ranges from 58 % (mildly humid) to 96 % (very humid) throughout a typical June, rarely dropping below 48 % (comfortable) and reaching as high as 100 % (very humid). The air is driest around June 1, at which time the relative humidity drops below 62 % (mildly humid) three days out of four; it is most humid around June 27, rising above 94 % (very humid) 3 days out of four in Figure 3 (Khan and Chatterjee 2016).

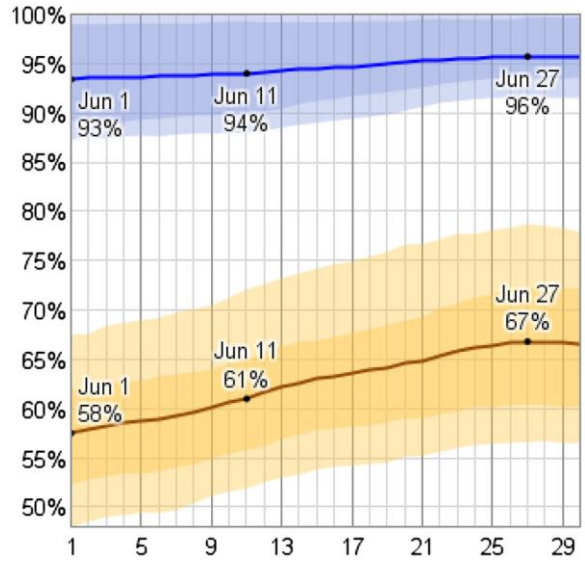

Fig. 3: The average daily high (blue) and low (brown) relative humidity (Khan and Chatterjee 2016)

The probability that precipitation is observed at this location varies throughout the month. Precipitation is most likely around June 30, occurring in 74 % of days. Precipitation is least likely around June 1, occurring in 56 % of days. Throughout June, the most common forms of precipitation are thunderstorms, light rain, and moderate rain. Thunderstorms are the most severe precipitation observed during 58 % of those days with precipitation. They are most likely around June 1, when it is observed during 39 % of all days (Khan and Chatterjee 2016). Light rain is the most severe precipitation observed during 24 % of those days with precipitation. It is most likely around June 30, when it is observed during 20 % of all days. Moderate rain is the most severe precipitation observed during 17 % of those days with precipitation. It is most likely around June 30, when it is observed during 16 % of all days in Figure 4 (Khan and Chatterjee 2016). Where T is the temperature (°C), t is time (s), z is the height (m), α is thermal diffusivity (ms-2), k is thermal conductivity (w/mK), ρ is density (g/cm3), c is heat capacity (J/kg K), and L is the height of bottom boundary (8 m). The related physical properties of urban open surface sand mixed soil and urban concrete surface are shown in Table 1. Therefore, the differential equation can be solved when the top boundary temperature and bottom boundary temperature are given. Since the surface temperature is influenced by many factors, it changes between different measurements points on the same ground surface. The difference may be significant, especially on concrete surfaces. Although the problem is assumed to be one-dimensional, the Vertical temperatures are influenced by the whole ground surface.

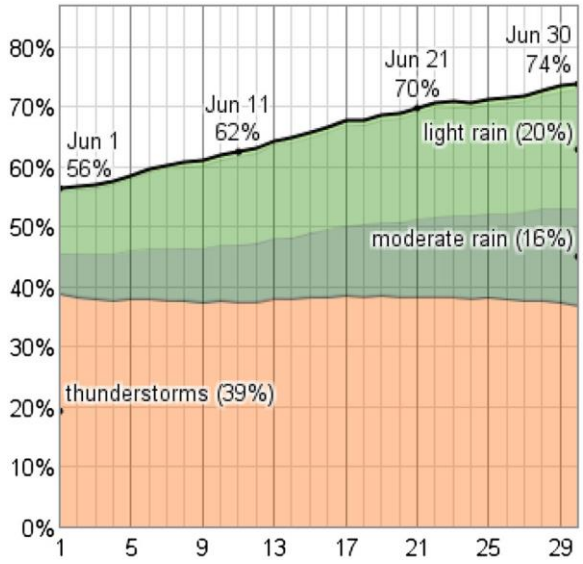

Fig. 4: The average daily Precipitation (Khan and Chatterjee 2016)

Vertical air temperatures are influenced by solar radiation, air moisture, wind speed, and environmental shelter, etc. Essentially, these factors act on the ground surface and then affect the vertical temperature field. To simulate the vertical temperature variations, we made three assumptions (Liu et al., 2011): a) the air is homogeneous, and as a result, heat only flows in a vertical direction; b) no surface heat source; c) air moisture is not considered. Therefore, the corresponding heat conduction equation is one-dimensional. In the Cartesian coordinates, the one-dimensional transient heat conduction differential equations are as follows (Equation 1 & 2).

$$\begin{cases} \dfrac{\partial T}{\partial t} = \alpha \dfrac{\partial^2 T}{\partial Z^2} & (0<z<L) \\ T(0,1)=\mu_1=\mu_2(t); T(L,t)=\mu_2(t) \end{cases} \quad (1)$$

$$\alpha = \frac{k}{\rho c} \quad (2)$$

Data Preparation, Processing, and Quantification techniques of the UHI

To quantify the UHI effectively, satellite Remote Sensing and GIS data play a crucial role. The datasets can be acquired from the electronic library (CLASS) of the National Oceanic and Atmospheric Administration (NOAA). LANDSAT, AVHRR data from NOAA-18 and NOAA-19 satellites are used for daytime because the satellite's time of overpass is near noontime when the

highest daily air temperatures occur. For nighttime, AVHRR data from the MetOp-A satellite can be used as the overpass time is around 22.30 local time (19.30 UTC).

Table 1: Physical properties of the urban concrete surface and urban open surface (sand) (Liu et al., 2011).

Surface	Dry Density (g/cm^3)	Thermal conductivity (w/mK)	Heat capacity (kJ/kg C)	Thermal diffusivity ($*10^{-6}$ m^2/s)	Relative humidity (%)
Urban open surface (sand)	1.52	0.71	0.8	0.81	85
Urban concrete surface	2.4	1.7	1.3	1.45	70

Satellite data processing

Temporal Landsat ETM+, OLI, or AVHRR data can be used to quantify the UHI and its impact assessment over Land use and environment. Landsat ETM+ or OLI data can be accessed freely from Earth explorer (USGS) with a spatial resolution of 30 ms. AVHRR thermal images (spatial resolution at 1.1 km) are used to map the thermal urban environment. All the Images should be geometrically corrected and radiometrically calibrated; radiometric calibration of the images involved the conversion of the raw digital number (DN) values (Saunders and Kriebel, 1988).

Urban atlas data processing

The Urban Atlas dataset is used to identify the urban, suburban, and rural regions. The aggregate land Use and Land cover type allows the spatial discrimination between the different urban land covers and also favors the spatially accurate assignment of the surface emissivity that corresponds to these urban land covers.

Land surface temperature (LST) extraction

Estimation of LST using AVHRR thermal infrared data is developed by Coll et al., (1994) (Equation 3). It requires the brightness temperatures in AVHRR channels 4 and 5, the mean emissivities, and the spectral emissivity difference in these channels. It also uses coefficients that depend on atmospheric moisture and surface temperature. These coefficients can be optimized according to the characteristics of a given area. The algorithm is described by the relation (Coll et al., 1994):

$$LST = T4 + [1 + 0.58\cdot(T4 - T5)] \cdot(T4 - T5) + 0.51 + \alpha\cdot(1 - E) - \beta\cdot(\Delta\varepsilon) \quad (3)$$

Where

T4 is the radiance temperature for channel 4 of AVHRR,

T5 is the radiance temperature for channel 5 of AVHRR,

E is the mean spectral emission coefficient for channels 4 and 5 (Equation 4).

$\Delta\varepsilon$ is the difference between the emission coefficients for channels 4 and 5

$$E = (\varepsilon 4 + \varepsilon 5)/2 \quad (4)$$

Where $\varepsilon 4$ is the surface-emission coefficient for channel 4

$\varepsilon 5$ is the surface-emission coefficient for channel 5

Values for E and $\Delta\varepsilon$ are taken from Stathopoulou et al., 2004 and are shown in Table 2 (Stathopoulou et al., 2004). Coefficients α and β depend on the amount of atmospheric water vapor in the area of the satellite image and from the temperature of the surface under observation. They may be described as a function of the brightness temperature (T4) which is recorded in channel 4 of the AVHRR and the precipitable water (PW) in the area (Caselles et al., 1997).

Table 2: Emissivity values by land cover type (Stathopoulou et al., 2004)

Land Cover Type	Mean Emissivity	Emissivity Difference
Urban	0.97	-0.007
Sub-urban	0.98	-0.003
Rural	0.989	0

Air temperature

Air temperatures shall be derived from AVHRR surface temperatures using a simple empirical relation with coefficients determined from the comparison of air temperatures observed at meteorological stations with coincident surface temperatures of the AVHRR pixels where the stations are located (Stathopoulou et al., 2004). Air temperature values at each station that are coincident with the satellite overpass time can be collected The relation is derived while applying to the AVHRR images to convert AVHRR surface temperatures into estimated air temperatures (Equations 5 & 6).

$$\text{Day: } Tair = 0.3896\cdot Ts + 15.313 \quad (5)$$

$$\text{Night: } Tair = 0.8246\cdot Ts + 6.2324 \quad (6)$$

Precipitable water (PW)

A study (Chrysoulakis et al., 2008) showed the relationship between the AVHRR temperature difference $\Delta T = T4 - T5$ (K) and the atmospheric precipitable water PW (cm) using daytime satellite data. They found this relationship is to be essentially linear and approximated by the following (Equation 7).

$$PW = 0.719\cdot\Delta T + 0.362 \quad (7)$$

For nighttime images, a relation was found more suitable (Choudhury et al., 1995), and for urban surfaces is expressed as Equation 8.

$$PW = 1.265\cdot\Delta T + 1.493 \quad (8)$$

Relative humidity (RH)

Relative humidity (RH %) is defined as the ratio of vapour pressure (e) to saturated vapor pressure (e_s) at the air temperature (T_a) expressed as a percent (Equation 9):

$$RH = 100 \times [\frac{e}{e_s T_a}] \quad (9)$$

Discomfort index (DI)

Thom's discomfort index (DI) is expressed by a simple linear equation based on dry-bulb (T_{dry}) and wet-bulb (T_{wet}) temperatures. Its original form is given as (Equation 10) (Choudhury et al., 1995).

$$DI(°F)=0.4(T_{dry}+T_{wet})+15 \quad (10)$$

If air temperature (*Ta*) as measured in degrees Celsius and relative humidity (*RH)* in % is given, DI can be computed by using the following Equation (11) (Choudhury et al., 1995).

$$DI(°C)= Ta – 0.55(1 - 0.01RH).(Ta -14.5) \quad (11)$$

The classes of DI are presented in Table 3 where it can be seen that the human discomfort increases as the Di values increases (Choudhury et al., 1995).

Table 3. Classes of discomfort index (DI) (Choudhury et al., 1995)

Class No.	DI (°C)	Discomfort conditions
1	DI<21	No discomfort
2	21≤DI<24	Less than 50% feels discomfort
3	24≤Di<27	More than 50% feels discomfort
4	27≤DI<29	Most of the population feels discomfort
5	29≤DI<32	Everyone feels severe stress
6	DI≥32	State of a medical emergency

In addition, the quantification process comprises the basic remote sensing image analyses for extraction of producing maps of Normalized Difference Built-up Index (NDBI) to measure the built-up index and Normalized Difference Vegetation Index (NDVI), to measure the vegetation index, which is used to attune the land surface temperatures.

Measuring vegetation index and built-up areas

Temporal satellite data can be used to segregate several land use classes as urban, suburban, and rural classes and assessment can be made based on long-term land-use changes over the changing climate and environment. Topographical evaluation can also be performed by observing the elevation conditions of the study area to their neighborhood area, temporal development, and urbanization process (pre, during, and post), and was conducted by comparative analyses of land-use changes, land surface temperatures, Normalized Difference Vegetation Index (NDVI), and Built-up Index (NDBI), and finally, a historical climate data comparison (rising sea levels and El Niño Southern Oscillation (ENSO) incidents) can be done to assess environmental risks.

Normalized different built-up index (NDBI)

The NDBI enhances the built-up features of the earth's surface. It is an automated mapping of urban built-up areas. Using the same rationing technique as NDVI, the building and urban area reflectivity are more concentrated at the middle-infrared (MIR) band compared to near-infrared (NIR) (Zha et al., 2003). Thus, the built-up land can be calculated using Equation (12).

$$NDBI= MIR-NIR / MIR+NIR \quad (12)$$

Normalised different vegetation index (NDVI)

The simplest form of vegetation index is a ratio of near-infrared (NIR) and red (R) reflectance, known as Simple Ratio (SR). For healthy living vegetation, this ratio will be high, due to the inverse relationship between vegetation brightness in the red and infrared regions of the spectrum. Based on geometrically corrected Landsat ETM+ or OLI images, the SR can be calculated using the reflectance of the near-infrared band (NIR) and is the reflectance of the red band (R) (Zha et al., 2003). The Normalized Difference Vegetation Index (NDVI) is the most commonly used. It can be calculated by using Equation (13):

$$NDVI= NIR-R / NIR+R \quad (13)$$

Future perspectives to adapt these techniques for the quantification of the UHI

Evaluation of Urban Landscape and Ecology

Landscape pattern is the spatial arrangement of landscape elements in different sizes and shapes. Analyzing landscape patterns is essential to monitor urban landscape spatial structure changes. Landscape pattern is a measure of an ecosystem's ability to prove habitat, prevent environmental degradation, and support other natural processes. To study the pattern change, different landscape metrics, including diversity index, shape index, patch density, mean of patch area distribution, and the landscape fractal dimension, are often adopted (Artis and Carnahan, 1982).

Urban Environmental Risk Assessment and Mapping

Urban Environmental risk assessment has become one of the primary contents of urban and rural ecological planning (Artis and Carnahan, 1982). The risk assessment is done through a correlation process and a thorough decision making on the results of the quantification process viz, the periodical increment of land surface temperature, urban agglomeration rate, Land use changing rate with a total urban population under risk zone. The detailed data quantification and analyses help to classify urban ecological units from high to low-risk zone on a local to regional scale.

Fig. 5. GUI of Urban Landuse and Environment-Software System (Artis and Carnahan, 1982).

Developing an effective Urban Landuse and Environment-Software System

Based on the aforementioned UHI quantification process and analyses, a software system can be developed for monitoring urban land use and environment effectively, including the basic modules and advanced modules for urban land use and environment details (Figure 5) (Artis and Carnahan, 1982). The software routines can be developed through Interactive Data Language (IDL). The system works with a collection of IDL source files and input of data and analytical results. To run these scripts, installation of a virtual machine of IDL 8.x or later shall be required. Output binary data are saved as Tagged Image File Format (TIFF) images, which are easy to open using professional Remote Sensing software or universal image processing software (Artis and Carnahan, 1982).

Adaptation and Mitigation Measures of the UHI

Mitigating and reducing the impacts contributed by the UHI and anthropogenic activities is a significant challenge to urban planners, designers, architects, and the local industry especially in the context of population and urban growth and the associated urban infrastructure. By implementing the following measures it is possible to improve the urban environment (Rose and Devadas, 2005). The importance of having urban green campaigns and infrastructures was suggested to influence the urban community environment. Outdoor participation leads to healthier lifestyles and helps to resolve the adverse effects of climate change, thus transforming the well-being of urban society and its environment. A major mitigation strategy, which has received global recognition and attention, is the escalation of surface cooling properties, which is the land surface albedo. Land surface albedo has a direct relationship with surface heat.

Recognising the issue

Built-up areas in cities create unique micro-climates as natural surfaces are replaced by artificial ones, affecting other local air temperatures. This makes cities particularly vulnerable to the impact of heatwaves. The phenomenon is called the ‘urban heat island effect’ and describes the increased temperature of the urban air compared to its rural surroundings.

Analysing the drivers

Rapid urban growth and high population density coupled with sealed surfaces, and a lack of green areas in combination with projected climate-induced changes exacerbate the risk of urban heat islands in cities. Built surfaces are composed of a high percentage of non-reflective construction materials. As a consequence, they tend to absorb a significant proportion of the incident radiation, which is released as heat. Additional causes of urban heat islands come from the residual heat of, for example, air conditioning and refrigeration systems, industrial processes, motorized traffic, and the obstruction of airflows. Climate change essentially increases the number of hot days for both urban and rural situations to a similar extent. However, the number of additional hot nights is

larger in cities. Urban areas store more heat during the day than greener rural areas and release this heat during the night.

Understanding the consequence

Climate projections show a substantial increase in periods of extreme heat in the region of South Asia. This, in turn, may reinforce the urban heat island effect in many urban agglomerations. Urban heat island effects go well beyond simple comfort issues for the population. Extreme heatwaves endanger human health and greatly affect everyday life, social activities, economic endeavors, and ecological systems.

A direct relationship has been established between peaks of urban heat island effects and heat-related illnesses and fatalities. Heatstrokes, heat exhaustion and heat cramps are some of the main stress incidents, while a large number of diseases may become worse – particularly for the elderly, chronically sick, very young, and socially isolated. This is mainly due to the lack of electricity and cooling systems – especially in many informal settlements – and lack of or damage to sanitation and water facilities.

Consequences include increasing stress on water resources from rising water demands and energy shocks as well as disruptions due to increased electricity demands caused by the growing use of air cooling systems. High temperatures can put infrastructures at risk by, for example, deforming roads and rail tracks, which in turn impede the supply of goods and the mobility of commuters into and out of the city.

Taking appropriate actions.

Local authorities should work towards mainstreaming measures against urban heat island effects in urban development plans, land use plans, and policies. To this end it is recommended to take a cross-sectoral approach, involving sectors like housing, public health, private sector building industry, transportation, and energy to be able to address the overarching nature of the challenge. Local authorities can initiate several actions to minimize a city's vulnerability to the effects of urban heat islands. First of all, local authorities should engage all relevant stakeholders in the planning and implementation of activities – also beyond the usual governance and management circles. It is also strongly recommended to engage those who are most vulnerable to heatwaves and urban heat island effects in the planning and policy-making processes, thereby identifying the most appropriate solutions and at the same time building capacity and increasing public awareness (Policy Pointer No. 2, 2013).

Early warning systems and educational campaigns to teach the general public to take precautionary actions during heat peaks are critical. Green infrastructure including improved vegetation and green building investments for natural cooling can play a crucial role to prepare the city on a long-term basis. This could include increasing the vegetation cover through reforestation as well as the number of parks and implementing vertical gardening to maximize the multiple vegetation benefits to alleviate temperature rises. Local authorities may consider other measures such as retrofitting public transport with ventilation as well as with white roofs to reduce solar heat gain; retrofitting buildings by adding light-colored roofs that provide a cooling effect; and increasing surface reflectivity to reduce radiation absorption of urban surfaces by using light-colored or white paint on the surface of construction materials. The following actions are summarized as a part of the adaptation measures of UHI (Policy Pointer No. 2, 2013).

- Reducing emissions by decongesting the roads.
- Use of passive techniques in designs for heating and cooling thereby reducing the anthropogenic heat generated.
- Increasing the vegetation cover by providing more trees to provide shelter and shade.
- Increased use of light-colored surfaces thereby reducing the absorption of radiation.
- A cool environment will provide less demand for energy, and thus, reduce pollution from power plants
- Trees and vegetation help to improve the transportation of air pollutants, such as oxides of sulfur and nitrogen; thus reducing air pollution.
- With cooler air temperatures, the formation of fog is less.
- Mainstream adaptation actions towards urban heat island effects across all sector departments.
- Maintain and extend the green infrastructure networks.
- Create awareness and guide how to behave during periods of extreme heat.
- Learn about best practices from your stakeholders and the most vulnerable.
- Use light-colored or white paint for sealed surfaces, buildings, and public transport vehicles.

Conclusions

The study gives a scientific approach to quantify the effects of the UHI over changing climate. It also gives a clear view to mitigate and respond to the climatic change and UHI for over urban land use and environment. Statistics shows, there is a substantial increase in urban air temperatures from the past, especially in all metropolitan and megacities. An increase in population, density, reduction in open spaces and green cover, increase in built-up spaces have proved to increase the air temperature. These

thermal changes deteriorate the urban environment causing health problems. Therefore Urban planners, designers, architects need to consider this urban climate while designing and planning cities.

This present study gives a clear view of the trend of temperature variation by deriving land surface temperature (LST) and simulating the process of Urban Land-use, environment, and LST. The correlation between different land uses/environments with LST shows positive or negative trends by showing the direction of the development pattern of urban development shortly and conversion into UHI by analyzing the trend from the past to present and present to the future development of settlement and impervious surface. A compact-town-like decentralization of urban areas (e.g., satellite towns) is, therefore, a possible way forward to prevent the formation of large-scale urban heat island effect in the future.

Acknowledgements

The author would like to convey special thanks to IMD, Kolkata for providing micro-meteorological in situ information. The author also expresses gratitude to the Principal Secretary and Joint Secretary to Govt. of West Bengal, DoDM & CD, and the District Magistrate, South 24 PGS. Finally, thanks to the anonymous reviewers for their careful review and insightful suggestions which led to a substantial improvement of the original paper.

Refences

Akyüz, E. (2021). The Development of Environmental Human Rights. International Journal of Environment and Geoinformatics , 8(2) , 218-225. DOI: 10.30897/ijegeo.839725.

Arnfield, A.J. (2003). Two decades of urban climate research: a review of turbulence, exchanges of energy and water, and the urban heat island. *International journal of climatology*, 23 (1), 1-26.

Artis, D.A. and Carnahan, W.H. (1982). Survey of emissivity variability in thermography of urban areas, *Remote Sensing of Environment*, 12 (4), 313–329.

Blocken, B., Stathopoulos, T., and Carmeliet, J. (2007). CFD simulation of the atmospheric boundary layer: wall function problems. *Atmospheric environment*, 41 (2), 238-252.

Brivio, P.A., Lechi, G., and Zilioli, E. (2006). Principles and methods ditelerilevamento, CittàStudiEdizioni, to Turin, 449-479.

Burak, S., Doğan, E., Gazioğlu, C. (2004). Impact of urbanization and tourism on coastal environment, Ocean Coast Manag., 47, 15-527.

Carlson, T.N. and Ripley, D.A. (1997). On the relation between NDVI, fractional vegetation cover, and leaf area index, *Remote Sensing of Environment*, 62 (3), 241–252.

Caselles, V., Coll, C., and Valor, E. (1997). Land surface emissivity and temperature determination in the whole HAPEX–Sahel area from AVHRR data, *International Journal of Remote Sensing*, 18, 1009–1027.

Choudhury, B.J., Dorman, T.J., and Hsu, A.Y. (1995). Modeled and observed relations between the AVHRR split window temperature difference and atmospheric precipitable water over land surfaces, *Remote Sensing of Environment*, 51, 281-290.

Chrysoulakis, N., Kamarianakis, Y., Xu, L., Mitraka, Z., and Ding, J. (2008). Combined use of MODIS, AVHRR and radiosonde data for the estimation of spatiotemporal distribution of precipitable water, *J. Geophys. Res*., 113, D05101.

Coll, C., Caselles, V., Sobrino, J. A., and Valor, E. (1994). On the atmospheric dependence of the split window equation for land surface temperature. *International Journal of Remote Sensing*, 15, 105–122.

Giannini, M. B., Belfiore, O. R., Parente, C., Santamaria, R. (2015). Land Surface Temperature from Landsat 5 TM images: comparison of different methods using airborne thermal data, *Journal of Engineering Science and Technology Review*, 8 (3), 83-90.

Kaya S, Basar UG, Karaca M, Seker DZ (2012) Assessment of urban heat islands using remotely sensed data. Ekoloji 21 (84):107-113.

Khan, A. and Chatterjee, S. (2016). Numerical simulation of urban heat island intensity under urban–suburban surface and reference site in Kolkata, India, Model. *Earth Syst. Environ.*, 2:71. DOI 10.1007/s40808-016-0119-5.

Liu, C., Shi, B., Tang, C., and Gao, L. (2011). A numerical and field investigation of underground temperatures under Urban heat island. *Build Environ.*, 46 (5), 1205–1210.

Marko, K., Zulkarnain, F., and Kusratmoko, E. (2016). Coupling of Markov chains and cellular automata spatial models to predict land cover changes (case study: upper CiLeungsi catchment area), IOP Conf. Ser.: *Earth Environ. Sci*., 47, 012032

Oke, T. R. (1973). City size and the urban heat island. *Atmospheric Environment*, 7 (8), 769-779.

Oke, T.R. and Maxwell, G.B. (1975). Urban heat island dynamics in Montreal and Vancouver. *Atmospheric Environment*, 9 (2), 191-200.

Pickett, S.T., Cadenasso, M.L., Grove, J.M., Nilon, C.H., Pouyat, R.V., Zipperer, W.C., and Costanza, R. (2008). Urban ecological systems: linking terrestrial ecological, physical, and socioeconomic components of metropolitan areas, *Urban Ecology*, 99-122.

Policy Pointer No. 2. (2013). Responding to Urban Heat Island Effects, *Asian Cities Adapt.*, 1-2.

Prasad, R. (2017). The urban heat island effect Rapid urbanisation increases temperatures, *The Hindu*

Rose, A.L. and Devadas, M.D. (2005). Effects Of Changing Landuse Patterns On Urban Heat Island

In Chennai, *World Sustainable Building Conference*, Tokyo (SB05Tokyo), 27-29 September, 3949-3952.

Saunders, R.W. Kriebel, K.T. (1988). An improved method for detecting clear sky and cloudy radiances from AVHRR data, *International Journal of Remote Sensing*, 9, 123–150.

Şekertekin, A., Kutoglu, Şh:, Kaya, Ş., Marangoz, AM. (2016). Monitoring the surface Heat Island (SHI) effects of industrial enterprises Int. Archiv. Photogrammetry, Remote Sens. Spatial Inform. Sci.,41, 289.

Snyder, W. C., Wan, Z., Zhang, Y., Feng, Y.Z. (1998). Classification based emissivity for land surface temperature measurement from space, *International Journal of Remote Sensing*, 19 (14), 2753–2774.

Sobrino, J. A., Caselles, V., and Becker, F. (1990). Significance of the remotely sensed thermal infrared measurements obtained over a citrus orchard, *ISPRS Photogrammetric Engineering and Remote Sensing*, 44 (6), 343–354.

Sobrino, J. A., Jiménez-Muñoz, J. C., and Paolini, L. (2004). Land surface temperature retrieval from LANDSAT TM 5, *Remote Sensing of Environment*, 90 (4), 434–440.

Stathopoulou, M., Cartalis, C., and Keramitsoglou, I. (2004). Mapping micro-urban heat islands using NOAA/AVHRR images and CORINE land cover: an application to coastal cities of Greece *International Journal of Remote Sensing*, 25 (12), 2301–2316.

Ülker, D., Bayırhan, İ., Mersin, K., Gazioğlu, C. (2020). A comparative CO2 emissions analysis and mitigation strategies of short-sea shipping and road transport in the Marmara Region, Carbon Management, 11(6): doi.10.1080/ 17583004. 2020.1852853.

Ülker, D., Ergüven, O., Gazioğlu, C. (2018). Socioeconomic impacts in a Changing Climate: Case Study Syria. International Journal of Environment and Geoinformatics, 5(1), 84-93.doi. 10.30897/ijegeo.406273.

Yang, L. (2014). Green Building Design: Wind Environment of Building. Shanghai: *Tongji University Press*.

Zha, Y., Gao, J., and Ni, S. (2003). Use of normalized difference built-up index in automatically mapping urban areas from TM imagery, *International Journal of Remote Sensing*, 24 (3), 583-594.